



## RESEARCH LETTER

10.1002/2014GL062900

## Key Points:

- Potholes in bedrock channels commonly evolve to an optimal aspect ratio of 2
- Theory shows that aspect ratios of 1–2 maximize bottom shear stress
- Computational fluid dynamics can help identify preferential scales of bed forms

## Correspondence to:

J. D. Pelletier,  
jdpellet@email.arizona.edu

## Citation:

Pelletier, J. D., K. E. Sweeney, J. J. Roering, and N. J. Finnegan (2015), Controls on the geometry of potholes in bedrock channels, *Geophys. Res. Lett.*, 42, 797–803, doi:10.1002/2014GL062900.

Received 17 DEC 2014

Accepted 22 DEC 2014

Accepted article online 29 DEC 2014

Published online 10 FEB 2015

## Controls on the geometry of potholes in bedrock channels

Jon D. Pelletier<sup>1</sup>, Kristin E. Sweeney<sup>2</sup>, Joshua J. Roering<sup>2</sup>, and Noah J. Finnegan<sup>3</sup>

<sup>1</sup>Department of Geosciences, University of Arizona, Tucson, Arizona, USA, <sup>2</sup>Department of Geological Sciences, University of Oregon, Eugene, Oregon, USA, <sup>3</sup>Department of Earth and Planetary Sciences, University of California, Santa Cruz, California, USA

**Abstract** Potholes (circular depressions carved into bedrock) are the dominant roughness elements in many bedrock channels. Here we show, using data from previous studies and new data from the Smith River, Oregon, that pothole depths increase in proportion to both the mean pothole radius (such that the most common pothole depth-to-radius ratio is 2) and the diameter of the largest clasts episodically stored in potholes. We present a theory for these observations based on computational fluid dynamics and sediment transport modeling of vortices in cylindrical cavities of different shapes and sizes. We show that the shear stress at the bottom of a pothole (which controls the rate of pothole growth) is maximized for potholes with a depth-to-radius ratio of approximately 1 and decreases nonlinearly with increasing depth-to-radius ratio such that potholes with depth-to-radius ratios larger than 3 are uncommon. Our model provides a mechanistic explanation for pothole shapes and sizes.

### 1. Introduction

Potholes are a common feature in bedrock channels. Their formation can be associated with a significant proportion of the total erosion in many bedrock channels. In many bedrock channels where potholes exist, they are the largest bed form type. Given that the size and shape of the largest bed forms exert a first-order control on water flow velocities via the drag they exert on the flow, the morphology of potholes likely exerts a primary control on turbulent flow structures, erosion rates and patterns, coarse sediment transport rates, and aquatic habitat diversity.

Potholes are thought to form via abrasive wear of initially minor channel bed depressions associated with mechanically weak zones such as intersections between vertically oriented joints [Ortega *et al.*, 2013], zones of locally enhanced weathering [Elston, 1917], remnants of other erosional bed forms such as grooves, and/or immobile rock/boulder obstructions [Goode and Wohl, 2010]. Eddies produced by shear flow enter these incipient depressions, at which point sediments entrained in the flow grind against the sides and bottoms of the depressions, resulting in pothole growth. The fact that potholes typically have smooth, vertical walls and often episodically store grinder particles with beveled edges within them supports the hypothesis that abrasion is an important element of pothole formation. Once potholes grow to sufficient depths, however, the increase in bed surface area and the associated increase in drag is thought to dissipate flow energy, thereby slowing the rate of pothole growth in a negative feedback [Johnson and Whipple, 2007; Johnson *et al.*, 2007].

Springer *et al.* [2005, 2006] developed a mathematical model that uses empirical data to grow potholes in radius and depth in a manner consistent with the scaling of these variables in field data. There is, however, currently no mechanistic model that links the fluid mechanics of swirling flow in potholes with pothole form. This paper is designed to fill that gap. Alexander [1932] divided potholes into three types: (1) eddy holes formed by abrasion in swirling flow, (2) gouge holes formed by the oblique impact of swift currents, and (3) plunge pool holes formed by falling water. This paper focuses exclusively on the eddy hole type of pothole.

### 2. Data on Pothole Geometry

Eddy-hole-type potholes exhibit an approximately linear relationship between mean radius,  $R$ , and depth,  $Z$ , from spatial scales of approximately 1 cm to 20 m (Figure 1). At the smallest spatial scales, the field data that we collected on the mean radius and depth (to the nearest centimeter) of 230 potholes on the bed of the

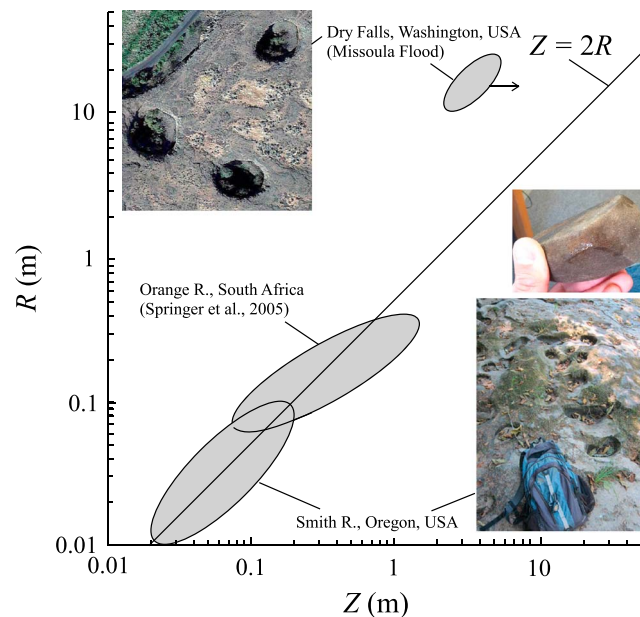


**Figure 1.** Schematic plot of the relationship between bedrock channel pothole radius and depth from potholes ranging in size from  $\sim 0.01$  m to  $\sim 20$  m. Ellipses show the approximate range of data values in each study area. The solid black line corresponds to  $\gamma = Z/R = 2$ . The top left image shows an aerial photograph of potholes approximately 15 m in radius near Dry Falls State Park, Washington (road for scale). The arrow in the plot indicates that depth measurements for these potholes are minima (due to progressive infilling over time since the Missoula Flood). The bottom right image shows potholes of Smith River (backpack for scale), Oregon, along with a photo of a grinder from one of the potholes with beveled edges shown.

Smith River, Oregon ( $43.78^{\circ}\text{N}$ ,  $123.81^{\circ}\text{W}$ ), document a linear relationship with a most common depth to radius or aspect ratio of 2 (Figure 2a). Springer *et al.* [2005, 2006] investigated the scaling of slightly larger potholes, i.e., those with radii of  $\sim 5$  cm to  $\sim 5$  m, on the bed of the Orange River, South Africa, and documented power law relationships between mean pothole radius and depth with exponents in the range of 0.57 to 0.85. Potholes that formed along the path of the Missoula (ice dam burst) flood near Dry Falls State Park, Washington, are approximately 15 m in radius and 5 m in depth (Figure 1) based on our measurements from U.S. Geological Survey aerial photographs and topographic maps with 10 ft (3.048 m) contour intervals. Depth is a minimum in the Missoula potholes due to partial infilling with sediment since the last Missoula flood that occurred in circa 14 ka. Collectively, these data indicate that pothole radius and depth are approximately proportional over the entire range of scales at which potholes occur, although significant deviations from proportionality can occur at

specific study sites and/or when considering data over a relatively narrow range of the pothole size spectrum [e.g., Springer *et al.*, 2005, 2006].

A linear relationship between pothole depth and radius implies an aspect ratio,  $\gamma = Z/R$ , that is independent of spatial scale. The aspect ratio of potholes has a most common value of 2 for our study site (i.e., the Smith River) (Figure 2b). The line  $Z = 2R$  plotted in Figure 1 that corresponds with a scale-independent aspect ratio of 2 is consistent with available data across a wide range of pothole sizes. Similar aspect ratios were also documented in potholes formed by wave action along coasts. Abbott and Pottratz [1969], for example, documented mean aspect ratios of between 1 and 2 in 140 potholes formed by coastal waves in Oahu, Hawaii, with larger aspect ratios characteristic of potholes formed in basalt and smaller aspect ratios in finely stratified volcanic tuff and calcareous beachrock.

We also measured the maximum and median intermediate-axis grain diameters of grinder particles found in 12 potholes of various sizes along the Smith River. These data show that the diameter of the largest clasts episodically stored in potholes is approximately equal to the pothole radius (Figure 2c). Median grain diameters showed no relationship to pothole diameter.

### 3. Theory and Modeling

Here we present a theoretical framework aimed at understanding the empirical data presented in Figures 1 and 2. This framework is based on equations for the fluid mechanics of swirling/vortical flows in cylinders and sediment transport in channels. We show that the shear stress exerted on the bottom of a cylindrical cavity is maximized for cavities with an aspect ratio of 1 and decreases rapidly with increasing aspect ratios such that potholes with aspect ratios significantly larger than the typical range of 1–3 are difficult to form. We further assume that potholes grow only if the coarsest sediments stored within them are episodically

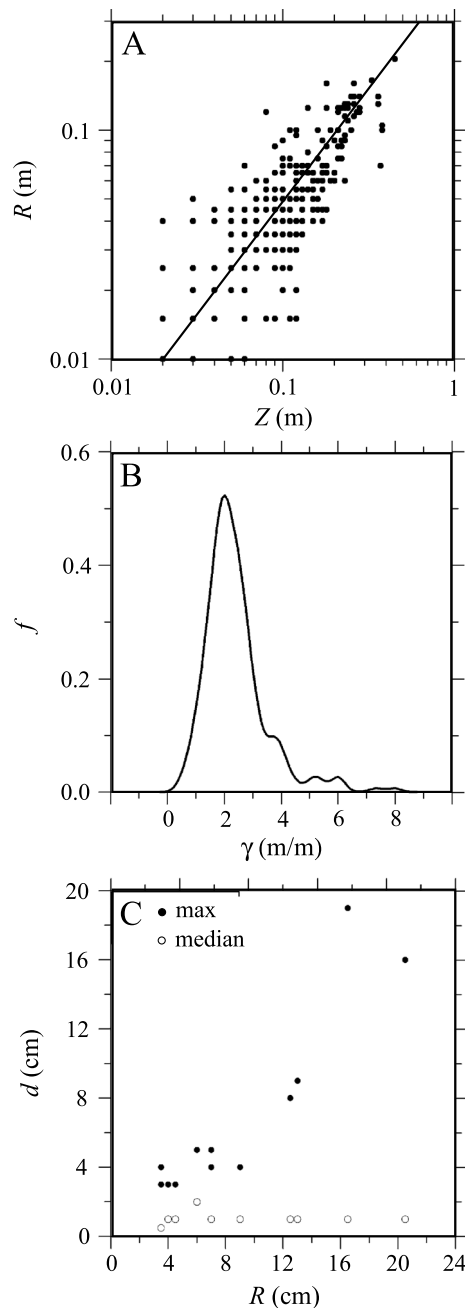


**Figure 2.** Plots of field measurements acquired along the Smith River, Oregon. (a) Plot of mean pothole radius versus depth (solid line shows  $\gamma = 2$ ), (b) probability density function showing the frequency of occurrence versus aspect ratio,  $\gamma$ , showing peak at  $\gamma = 2$ , and (c) plot of maximum and median intermediate-axis grain diameter versus mean pothole radius.

entrained (since, in the absence of entrainment, sediments will protect the bottom and lower sidewalls from erosion). Using this assumption, we show that the pothole radii scale with the product of the characteristic flow depth and channel slope.

### 3.1. Controls on the Aspect Ratios of Potholes

We used the 2013 version of the PHOENICS computational fluid dynamics (CFD) modeling code [Ludwig, 2011] to estimate the time-averaged flow velocities and shear stresses in a closed cylindrical cavity driven by an upper rotating endwall. In natural channels, shear flow generates open-channel eddies that induce vortical flow within the pothole from above. In our simplified model, the rotating endwall mimics the action of such open-channel eddies.

PHOENICS uses a finite-volume scheme to solve simultaneously for the pressure and velocity of turbulent flows in arbitrary geometries. PHOENICS is capable of employing many different turbulence schemes from the relatively simple  $k-\epsilon$  turbulence closure scheme to more sophisticated large-eddy simulation schemes. In this study we used the renormalization group variant of the  $k-\epsilon$  closure scheme due to Yakhot and Orszag [1986]. This scheme retains the simplicity of  $k-\epsilon$  closure but results in significant improvements in modeling highly sheared/separated flows.

Our default computational grid consists of a 3-D polar coordinate system with 60 cells in each direction (radial, azimuthal, and vertical) and a radius of 0.2 m (i.e., comparable to the largest potholes at the Smith River study site). The depth of the cylinder was varied from 0.1 m to 1.4 m, yielding aspect ratios from 0.5 to 7. The walls were assumed to be hydraulically rough boundaries (an assumption appropriate for most bedrock channel floods [Richardson and Carling, 2005]) with a roughness length of  $10^{-3}$  m. We repeated all of our calculations with a coarser grid (i.e., 30 cells in all directions). Minor differences in the results as a function of grid resolution occurred; these are due to the presence of a fluid-mechanical discontinuity at the intersection of the rotating endwall and the top of the static endwall (an issue explored in detail by Muite [2004]). This issue only affects the absolute values of shear stress predicted by the model; the relative shear stresses at different aspect ratios did

not depend on grid resolution. The results were also shown to be qualitatively robust with respect to the absolute size of the pothole, i.e., we repeated the calculations for a pothole of radius fixed at 1 m and found that the relative flow velocities and shear stresses varied with aspect ratio in the same manner as the simulations presented here.

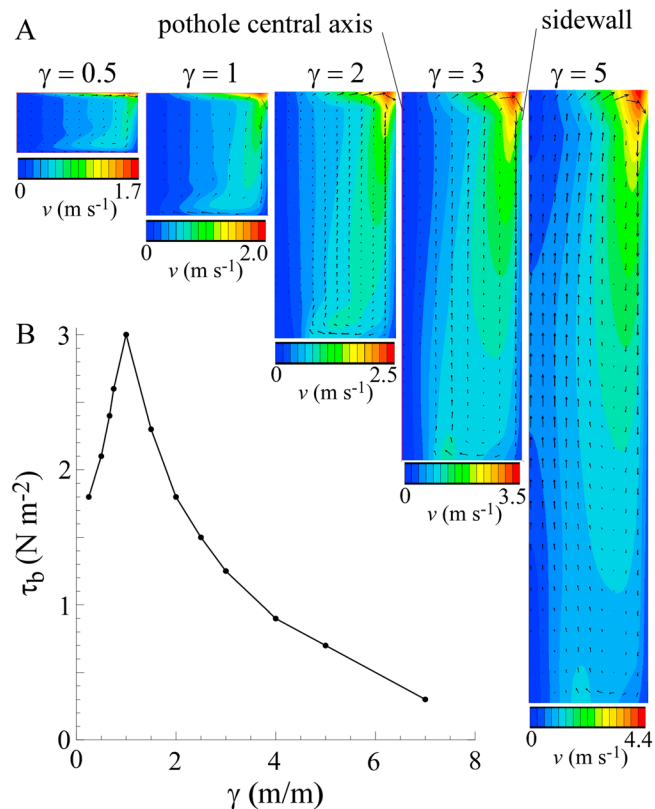


**Figure 3.** Results of the CFD modeling. (a) Color maps illustrate the flow velocity,  $v$ , in potholes with a radius of 0.2 m but different depths such that aspect ratios vary from 0.5 to 5. (b) Plot of the mean bottom shear stress,  $\tau_b$ , a proxy for the rate of pothole growth. The maximum  $\tau_b$  value occurs for cylinders with an aspect ratio,  $\gamma$ , of 1.

We assumed a fixed fluid kinetic energy per unit volume of  $100 \text{ J m}^{-3}$  across all model runs (i.e., pothole aspect ratios). The endwall rotation rate (a required input to the model) was varied iteratively to achieve this specific value of kinetic energy per unit volume, which corresponds to an endwall rotation rate of  $10 \text{ rad s}^{-1}$  and a maximum flow velocity of  $2 \text{ m s}^{-1}$  for the  $\gamma = 1$  case. Driving the flow with a fixed kinetic energy per unit volume assumes that the energy density within the flow is conserved within the turbulent inertial range of spatial scales (i.e., the range between the largest scales where power is input and the smallest scales where power is dissipated viscously). This aspect of turbulent flows follows from the scaling laws of Kolmogorov [1941] (e.g., see Ecke [2005] for more explanation), which were originally developed for isotropic turbulence but have nonetheless been verified for open-channel flows [Yokosi, 1967; Sukhodolov et al., 1998; Singh et al., 2010]. The effect of assuming a fixed fluid kinetic energy per unit volume is that the endwall rotation rate is modestly lower for shallow potholes

compared with deep potholes, reflecting the fact that shallow potholes exert greater drag per unit volume on the swirling flow within them compared with deeper potholes.

Endwall rotation generates a maximum velocity at the outermost edge of the top of each cylinder (Figure 3a; since the flows are axisymmetric, only a radial half cross-section from the center to the sidewall is shown). The dominant velocity component is azimuthal (i.e., a vortex). Flow velocities decrease toward the center and bottom of each cylinder due to the drag associated with the static bottom wall and sidewall. However, there is also a secondary axial and radial flow established in which fluid travels down the stationary sidewall, moves in along the bottom wall, and returns up along the center of the pothole (shown using in-plane velocity vectors superposed on the color maps in Figure 3a). This is the secondary flow pattern expected based on experiments of flow in potholes [e.g., Alexander, 1932] and previous fluid-mechanical studies of flow in driven cylindrical cavities [Pao, 1972; Khalili and Rath, 1994; Hills, 2001; Muite, 2004; Lopez, 1998, 2012].

We adopt the mean bottom shear stress,  $\tau_b$ , as a proxy for the pothole growth rate (including deepening and widening). Figure 3b illustrates how  $\tau_b$  varies with aspect ratio, and notably,  $\tau_b$  is maximized for aspect ratios of  $\sim 1$ . Our results also demonstrate that the mean bottom shear stress decreases nonlinearly with increasing aspect ratio for large aspect ratios: the bottom shear stress of a cylinder with an aspect ratio of 7 is less than 10% of the value for a cylinder with an aspect ratio of 1. The rotating endwall generates kinetic energy that penetrates only so far into the cylinder because sidewall drag triggers vortex breakdown in large aspect ratio cylinders. By contrast, small aspect ratios cylinders have a lower bottom shear stress compared with the  $\gamma = 1$  case because the small separation distance (and hence drag) between endwalls limits vortex development in such geometries.

### 3.2. Controls on the Absolute Sizes of Potholes

In this section we assume, based on measurements presented in Figure 2b, that potholes episodically store sediments with a maximum size comparable to the pothole radius. We further assume that pothole growth

requires that such clasts be episodically entrained, because otherwise the bottom of the pothole would be protected from erosion. Based on these assumptions, the analysis in this section implies that a linear relationship exists between the absolute sizes of potholes (not just their aspect ratios) and the characteristic depths of flows in the channel in which they form.

The most basic constraint on eddy-hole-type pothole sizes is the range of eddy sizes. Turbulent eddies in rivers occur in size from  $\sim 1$  mm [Yokosi, 1967] to the physical dimensions of the channel in flood ( $\sim 10$  m for the Smith River). As Figure 2 demonstrates, the vast majority of potholes on the Smith River have radii in the range of 5 to 10 cm, i.e., a much narrower range of sizes than the eddies in the channel. This suggests that other constraints are at work besides the range of eddy sizes in the channel flow.

To entrain sediment from the bottom of the pothole, it is necessary that the Rouse number (defined as the ratio of the settling velocity,  $w_s$ , to the product of the von Karman constant,  $\kappa$  (0.41), and the bed shear velocity,  $u_*$ ) be smaller than 7.5 [e.g., Julien, 1998], i.e.,

$$\frac{w_s(d)}{\kappa u_*} < 7.5, \quad (1)$$

where  $d$  is grain diameter. The appearance of  $d$  in equation (1) serves to emphasize that the settling velocity is primarily a function of grain diameter. Here we use the empirical equation of *Ferguson and Church* [2004] to estimate settling velocity, assuming parameter values appropriate for sieve diameters of natural grains. For particle diameters much larger than  $10^{-3}$  m, the settling velocity ( $\text{m s}^{-1}$ ) in water is approximately equal to 4.65 times the square root of the grain diameter (m), i.e.,

$$w_s = \frac{16.17d^2}{1.8 \cdot 10^{-5} + 3.48d^{3/2}} \approx 4.65d^{1/2} \text{ for } d \gg 10^{-3} \text{ m}. \quad (2)$$

Substituting  $R$  for  $d$  in equation (1) (based on the assumption that the largest grains are comparable in size to the pothole radius) and using the depth-slope product to estimate the bed shear velocity gives, for  $R \gg 10^{-3}$  m, a lower bound for the characteristic flow depth required to form a pothole of radius  $R$

$$h > 0.23 \frac{R}{S} \quad (3)$$

where  $h$  is the flow depth and  $S$  is the channel slope. Equation (3) implies that for channel slopes  $\sim 10^{-1}$  m/m, the necessary flow depth required to form potholes is approximately twice the pothole radius.

If we further assume that potholes form most rapidly when the largest clasts stored in potholes are transported as bed material load, this places an approximate upper bound of  $2.2R/S$  on the formative flow depth associated with a pothole of radius  $R$  in a channel of slope  $S$  since deeper flows would put material in wash load. This result is obtained using a variant of the inequality in equation (1) in which the Rouse number is required to be larger than 0.8 (i.e., the threshold for 100% wash load) instead of being smaller than 7.5 (i.e., entrainment). This upper bound does not imply that wash load does no abrasive work. Rather, it simply suggests that the occasional exchange of sediment between a pothole and the coarsest clasts that might occupy the pothole promotes pothole development.

#### 4. Discussion

Our model predicts a fastest growth rate for potholes with  $\gamma = 1$ , while data indicate that the most common value is 2. Several factors could explain this difference. First, many potholes are partially filled with sediment clasts (the largest of which is comparable to the pothole radius in the case of the Smith River), so many potholes with  $\gamma = 2$  have an effective  $\gamma$  value (taking stored sediment into account) of close to 1. Second, our model results suggest that potholes with  $\gamma$  values in the 0–2 range will continue to deepen such that the most common aspect ratio is likely larger than 1 but smaller than 3, the point at which the bottom shear stress falls to a small fraction of its peak value. Third, additional criteria besides fluid mechanics may control pothole aspect ratios. For example, small  $\gamma$  value potholes are likely to be less efficient at trapping sediments during low flows that can promote pothole formation when mobilized during high flows, thus pushing the optimal growth rate for potholes higher than 1. Fourth, vortices in potholes are subject to streamwise shear stresses that can trigger horizontally oriented eddies, the behavior of which may depend on aspect ratio differently than the vertically oriented eddies considered here. For example, studies of 2-D flow in

bed cavities interacting with open-channel flows [e.g., Brandeis, 1982] show that the velocity of horizontally oriented eddies in such cavities is maximized for  $\gamma = 2$ . Therefore, to the extent that pothole formation depends on both horizontal and vertically oriented eddies, the optimal growth rate for potholes can be expected to occur at  $\gamma$  values between 1 and 2. Further research is needed to explore these hypotheses. The model of this paper is nonetheless an important first step toward a mechanistic model of pothole formation.

Insufficient data exist to rigorously compare equation (3) to pothole data. Specifically, we lack data relating pothole size to formative flow depths. However, all else being equal, it is clear from Figure 1 that channels with deeper characteristic flows have larger potholes. For example, 100 m deep flows (e.g., Missoula Flood) generate potholes that are up to approximately 20 m in radius, while flows along the Smith River, where flood depths are  $\sim 1$  m, generate potholes in the range of a few centimeters to a few decimeters in radius. As such, the linear scaling between the absolute size of potholes and characteristic flow depths predicted by equation (3) is broadly consistent with available data.

Our analysis assumes no limit to the size of clasts provided to the channel. That is, we assume that larger potholes will episodically trap clasts comparable in size to the radius of the pothole regardless of how large potholes become. Undoubtedly, this assumption does not apply to all channels, but we know that even for the largest floods on Earth (e.g., the Missoula flood), clasts comparable in size to the largest pothole radius (i.e., 20 m) were transported in the flow [Baker, 1973] and hence were likely episodically stored in potholes.

## 5. Conclusions

Potholes are a fundamental fluvial bed form type whose formation represents an important erosion process in many bedrock channels. Here we presented a preliminary mechanistic model for pothole formation. We showed that the bottom shear stress in a pothole achieves a maximum for potholes with  $\gamma = 1$  and decreases rapidly with increasing  $\gamma$  values. This predicted dependence of growth rate on aspect ratio is broadly consistent with data, in which potholes with aspect ratios in the range of 1–3 are most common. Our model and the new data we provide on potholes in the Smith River highlight the important role played by the largest grains episodically stored in the pothole in controlling the size of potholes. In the model, deeper flows and/or steeper channel beds promote larger potholes via the requirement that sediment stored in the pothole be episodically entrained.

### Acknowledgments

We thank Joel Johnson and Phairot Chatanantavet for helpful reviews. All data and model results can be obtained by request from J.D.P.

The Editor thanks Phairot Chatanantavet and an anonymous reviewer for their assistance in evaluating this paper.

### References

- Abbott, A. T., and S. W. Pottratz (1969), Marine pothole erosion, Oahu, Hawaii, *Pac. Sci.*, *23*, 276–290.
- Alexander, H. S. (1932), Pothole erosion, *J. Geol.*, *40*, 305–337, doi:10.1086/623954.
- Baker, V. R. (1973), Palaeohydrology and sedimentology of Lake Missoula flooding in eastern Washington, *Geol. Soc. Am. Spec. Pap.*, *144*, 1–79.
- Brandeis, J. (1982), Flow separation in shear-layer-driven cavities, *Am. Inst. Aeronaut. Astronaut. J.*, *20*(7), 908–914, doi:10.2514/3.51148.
- Ecke, R. (2005), The problem of turbulence: An experimentalist's perspective, *Los Alamos Sci.*, *29*, 124–141.
- Elston, E. D. (1917), Potholes: Their variety, origin and significance, (I), *Sci. Mon.*, *5*, 554–567.
- Ferguson, R. I., and M. Church (2004), A simple universal equation for grain settling velocity, *J. Sediment. Res.*, *74*(6), 933–937, doi:10.1306/051204740933.
- Goode, J. R., and E. Wohl (2010), Coarse sediment transport in a bedrock channel with complex bed topography, *Water Resour. Res.*, *46*, W11532, doi:10.1029/2009WR008135.
- Hills, C. P. (2001), Eddies induced in cylindrical containers by a rotating end wall, *Phys. Fluids*, *13*, 2279–2286, doi:10.1063/1.1384470.
- Johnson, J. P., and K. X. Whipple (2007), Feedbacks between erosion and sediment transport in experimental bedrock channels, *Earth Surf. Processes Landforms*, *32*, 1048–1062, doi:10.1002/esp.1471.
- Johnson, J. P. L., K. X. Whipple, and L. S. Sklar (2007), Contrasting bedrock incision rates from snowmelt and flash floods in the Henry Mountains, Utah, *Geol. Soc. Am. Bull.*, *122*, 1600–1615, doi:10.1130/B30126.1.
- Julien, P. Y. (1998), *Erosion and Sedimentation*, pp. 280, Cambridge Univ. Press, New York.
- Khalili, A., and H. J. Rath (1994), Analytical solution for a steady flow of enclosed rotating disks, *Zeitschrift Mathematik Physik*, *45*, 670–680, doi:10.1007/BF00991903.
- Kolmogorov, A. N. (1941), Energy dissipation in locally isotropic turbulence, *Dok. Akad. Nauk. SSSR*, *32*, 19–21.
- Lopez, J. M. (1998), Characteristics of endwall and sidewall boundary layers in a rotating cylinder with a differentially rotating endwall, *J. Fluid Mech.*, *359*, 49–79, doi:10.1017/S002211209700829X.
- Lopez, J. M. (2012), Three-dimensional swirling flows in a tall cylinder driven by a rotating endwall, *Phys. Fluids*, *24*, 014101, doi:10.1063/1.3673608.
- Ludwig, J. C. (2011), PHOENICS-VR reference guide, CHAM Ltd., London, U.K., digital document. [Available at <http://www.cham.co.uk/documentation/tr326.pdf>.]
- Muite, B. K. (2004), The flow in a cylindrical container with a rotating end wall at small but finite Reynolds number, *Phys. Fluids*, *16*, 3614–3626, doi:10.1063/1.1779567.

- Ortega, J. A., M. Gomez-Heras, and R. Perez-Lopez (2013), Multiscale structural and lithologic controls in the development of stream potholes on granite bedrock rivers, *Geomorphology*, *204*, 588–598, doi:10.1016/j.geomorph.2013.09.005.
- Pao, H.-P. (1972), Numerical solution of the Navier-Stokes equations for flows in the disk-cylinder system, *Phys. Fluids*, *15*, 4–11, doi:10.1063/1.1693752.
- Richardson, K., and P. A. Carling (2005), A typology of sculpted forms in open bedrock channels, *Geol. Soc. Am. Spec. Pap.*, *392*, 1–108, doi:10.1130/0-8137-2392-2.1.
- Singh, A., F. Porté-Agel, and E. Fofoula-Georgiou (2010), On the influence of gravel bed dynamics on velocity power spectra, *Water Resour. Res.*, *46*, W04509, doi:10.1029/2009WR008190.
- Springer, G. S., S. Tooth, and E. E. Wohl (2005), Dynamics of pothole growth as defined by field data and geometrical description, *J. Geophys. Res.*, *110*, F04010, doi:10.1029/2005JF00032.
- Springer, G. S., S. Tooth, and E. E. Wohl (2006), Theoretical modeling of stream potholes based upon empirical observations from the Orange River, Republic of South Africa, *Geomorphology*, *82*, 160–176, doi:10.1016/j.geomorph.2005.09.023.
- Sukhodolov, A., M. Thiele, and H. Bungartz (1998), Turbulence structure in a river reach with sand bed, *Water Resour. Res.*, *34*(5), 1317–1334, doi:10.1029/98WR00269.
- Yakhot, V., and S. A. Orszag (1986), Renormalization group analysis of turbulence. 1. Basic theory, *J. Sci. Comput.*, *1*, 3–51, doi:10.1007/BF01061452.
- Yokosi, S. (1967), The structure of river turbulence, *Bull. Dis. Prev. Res. Inst.*, *17*(2), 1–29.